Materials Science and Engineering A 527 (2010) 708–714

Contents lists available at ScienceDirect

Materials Science and Engineering A

journal homepage: www.elsevier.com/locate/msea

Effects of heat input on tensile properties and fracture behavior of friction stir welded Mg–3Al–1Zn alloy

J. Yang, B.L. Xiao, D. Wang, Z.Y. Ma*

Shenyang National Laboratory for Materials Science, Institute of Metal Research, Chinese Academy of Sciences, 72 Wenhua Road, Shenyang 110016, China

ARTICLE INFO

Article history:
Received 24 June 2009
Received in revised form 20 August 2009
Accepted 22 September 2009

Keywords:
Friction stir welding
Magnesium
Texture
Properties
Fracture

ABSTRACT

6.3 mm thick Mg–3Al–1Zn plates were friction stir welded with different shoulder dimensions at a traverse speed of 100 mm/min and a rotation rate of 800 rpm. With increasing the heat input by enlarging the shoulder diameter from 18 to 24 mm, the tensile strength of the welds tended to increase and the elongation was significantly improved, and the facture location shifted from the thermomechanically affected zone (TMAZ) in the advancing side to the stir zone. The highest ultimate tensile strength of the welds was obtained by using the shoulder 24 mm in diameter and reached up to 86% of the base material. The variation in the mechanical properties and fracture location was mainly attributed to the texture change in the TMAZ. However, the hardness profiles of the welds were hardly influenced by the shoulder size.

1. Introduction

Magnesium alloys are very attractive for structural applications for their low density, high specific strength and modulus. Problems with the conventional fusion welding, limiting the use of the magnesium alloys, could be eliminated by friction stir welding (FSW), which is a solid state welding process [1]. Nowadays, FSW has been widely used to join the magnesium alloys, such as Mg–Al–Zn [2–7], Mg–Zn–Y [8,9], and Mg–Al–Ca [10].

AZ31 is one of widely used wrought magnesium alloys with a good combination of strength and ductility. In the past few years, several investigations have been conducted to weld AZ31 alloy plates or sheets by FSW and defect free FSW AZ31 joints have been obtained by many researchers [2–7]. Because of the poor plastic deformability, generally, high heat input is necessary to obtain the high-quality joints by FSW. For example, Lee et al. [2] reported that defect free FSW AZ31 joints were obtained at rotation rates higher than 1600 rpm. However, higher ratio of rotation rate/traverse speed (ω/v), i.e. higher heat input, was reported by Gharacheh et al. [7] to decrease the tensile properties of FSW AZ31 joints. More recently, Afrin et al. [5] reported that the yield strength (YS) and ultimate tensile strength (UTS) of FSW AZ31 joints increased with increasing welding speed, i.e. with decreasing the FSW heat input. These investigations indicate that the FSW heat input exerted significant effects on the weldability of the magnesium alloys and the mechanical properties of the FSW joints.

The failure of the FSW AZ31 joints was generally attributed to two reasons in these studies. Some investigations [4,5] pointed out that the oxide layers resulted in the failure of the FSW samples with reduced mechanical properties since the oxides were found in the fracture surfaces. However, as easily oxidized alloys, it is difficult to determine if the oxides on the fracture surface of the FSW magnesium alloy joint resulted from the joint itself or the oxidation caused by the environment. On the other hand, many researches [11–14] attributed the failure of the FSW AZ31 joints to the texture variation during FSW.

Recently, the texture of FSW/FSP AZ (Mg–Al–Zn) series alloys was examined by means of X-ray diffraction (XRD), neutron diffraction and electron backscattered diffraction (EBSD) [11–15]. Park et al. [11,15] reported that the failure location of FSW AZ61 joint was associated with the texture because the texture varied in various weld zones. For the FSW AZ31 joints, texture was considered as a major factor for the failure, and the joints failed along the plane with higher Schmid factor [11], or the fracture was due to the plastic incompatibility made by the orientation difference between the stir zone (SZ) and the transition region [14]. However, these studies were mostly conducted under a single welding condition. Little attention was paid to the effect of the welding conditions on the fracture behavior of the FSW magnesium alloy joints.

In this study, 6.3 mm thick hot-rolled AZ31 plates were subjected to FSW using the tools with different shoulder diameters. The purpose of this study is to understand the effects of heat input on the mechanical properties and fracture behavior of the FSW magnesium alloy joints.

* Corresponding author. Tel.: +86 24 83978908; fax: +86 24 83978908.
E-mail address: zyma@imr.ac.cn (Z.Y. Ma).

0921-5093/$ – see front matter © 2009 Elsevier B.V. All rights reserved.
doi:10.1016/j.msea.2009.09.044

Table 1
Shoulder diameters used in this study and grain size in various zones of FSW AZ31 joints.

Sample no.	Shoulder diameter, mm	Grain size in SZ, μm	Grain size in TMAZ, μm
1	18	10	13
2	20	13	14
3	24	19	16

2. Experimental

Hot-rolled AZ31 magnesium alloy plate 6.3 mm in thickness was used in this study. Three FSW tools with the same cylindrical threaded pin having a diameter of 8 mm and a length of 5.9 mm, but with different shoulder diameters of 18, 20 and 24 mm, respectively, were used (Table 1). FSW was conducted along the rolling direction (RD) at a traverse speed of 100 mm/min and a rotation rate of 800 rpm, with a tool tilt angle of 2.8°. Three directions of the rolled plate were named as normal direction (ND), transverse direction (TD), and RD, respectively, as shown in Fig. 1.

Samples for microstructure examinations were cut perpendicular to the RD. After being mechanically ground and polished, the samples were etched with an etching reagent consisting of 4.2 g picric acid, 10 ml acetic acid, 10 ml H_2O and 70 ml ethanol. Microstructures were examined by optical microscopy (OM). The pole figure of the SZs and the diffraction intensity of the thermo-mechanically affected zones (TMAZs) were detected by XRD using CuKα radiation, respectively. The samples for XRD were cut perpendicular to the RD for both base material (BM) and FSW joints, as shown in Fig. 1. Furthermore, the SZ was observed by transmission electron microscope (TEM). TEM samples were cut perpendicular to the RD. Thin foils for TEM were ion-milled by PIPS691 at a voltage of 4 kV.

The hardness profiles of the transverse cross-section along the center line of the plates were measured on a Vickers hardness tester with a 300 g load for 13 s. Transverse tensile specimens with a gauge length of 40 mm and a gage width of 10 mm were machined, and tested at a strain rate of $1 \times 10^{-3}\,s^{-1}$ by using Zwick/Roell Z050 tester. Besides, mini tensile specimens with a gauge length of 2.5 mm, a gauge width of 1.4 mm, and a gauge thickness of 1.0 mm were cut in the SZ perpendicular to the welding direction (as shown in Fig. 2b), and tested with a strain rate of $1 \times 10^{-3}\,s^{-1}$ by using Instron 5848 tester. The results of tensile tests were taken from three and five specimens, respectively, for the transverse tensile and mini tensile tests. The fracture surface of transverse tensile specimens was observed by a scanning electron microscope (SEM).

3. Results and discussion

3.1. Microstructure

The typical cross-section photographs of the FSW AZ31 samples are shown in Fig. 2. The FSW samples had the similar shape of the

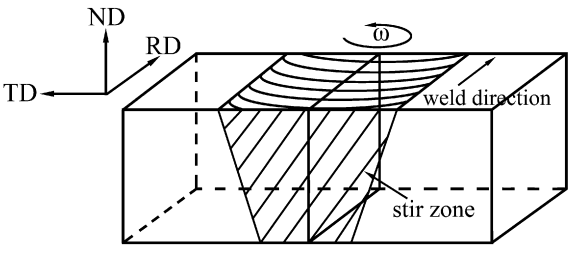

Fig. 1. Schematic illustration of the directions for the FSW and the selected area for analysis of XRD.

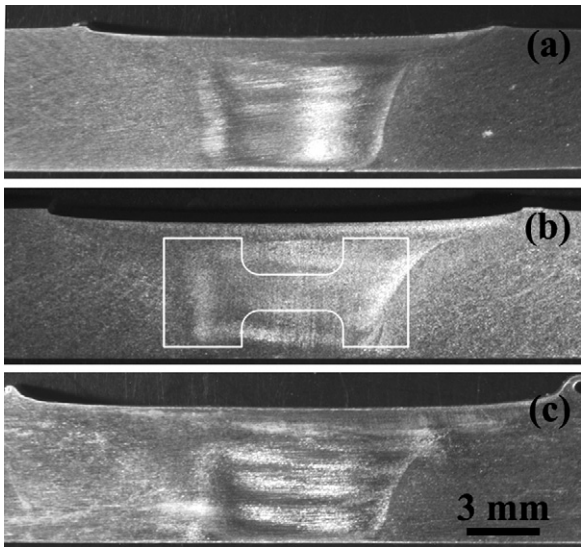

Fig. 2. The typical cross-section photograph of AZ31 FSW specimens: (a)–(c) sample 1–sample 3 (The advancing side of the weld is on the right.)

SZs. With different shoulder dimensions, defect free joints were produced. Similar to previous reports [4,5], four microstructural zones, i.e. SZ, TMAZ, heat-affected zone (HAZ), and BM zone, were identified for the FSW AZ31 samples. Fig. 3a shows a cross-sectional micrograph of the AZ31 BM. The BM shows inhomogeneous grains and numerous twins, which are the typical rolled microstructure of the magnesium alloys. The average grain size of the BM was determined to be about 21 μm. Fig. 3b–d shows the microstructure of the SZs of the FSW AZ31 joints prepared with various shoulder dimensions. The SZs were characterized by equiaxed and uniform grains, indicating the occurrence of dynamic recrystallization (DRX) in the SZs. For the lowest heat input with the smallest shoulder diameter of 18 mm, the grain of the SZ was the finest, which was about 10 μm and half of the BM. With increasing the shoulder diameter to 20 and 24 mm, the increased heat input resulted in the increase of the grain size in the SZ to about 13 and 19 μm (Table 1). Furthermore, it is noted that the twins were seldom observed in the SZs.

It is clear that the grains of the SZs increased with increasing the heat input. In several previous researches [11,16], authors claimed that the SZ was exposed to a temperature higher than the recrystallization temperature but lower than the melting point. So the material in the SZ underwent DRX under the stirring effects of the tool, producing fine and equiaxed grains, and the twins disappeared as well. Increasing the heat input produced higher process temperature in the SZ during FSW, this resulted in the increase in the size of the recrystallized grains due to the coarsening of the newly nucleated grains at higher temperatures.

Microstructures of the TMAZs at the advance side are displayed in Fig. 4. Nearly equiaxed grains were observed in the TMAZs for all the FSW samples, which are quite different from the observations made in FSW aluminum alloys where elongated grains along the flow line were revealed in the TMAZs [17]. Furthermore, it is noted that the grain microstructures in the TMAZs were different from those in the BM and SZs. According to a previous report [11], the grains in the TMAZ of FSW AZ61 joint were considered to experience DRX to form equiaxed grains due to the low recrystallization temperature of about 523 K. Therefore, based on the grain microstructures in the TMAZs of the present FSW AZ31 joints, it is concluded that DRX occurred in the TMAZs under the combined effects of deformation and heating, resulting in the generation of nearly equiaxed grains. Furthermore, it is noted that the grain size

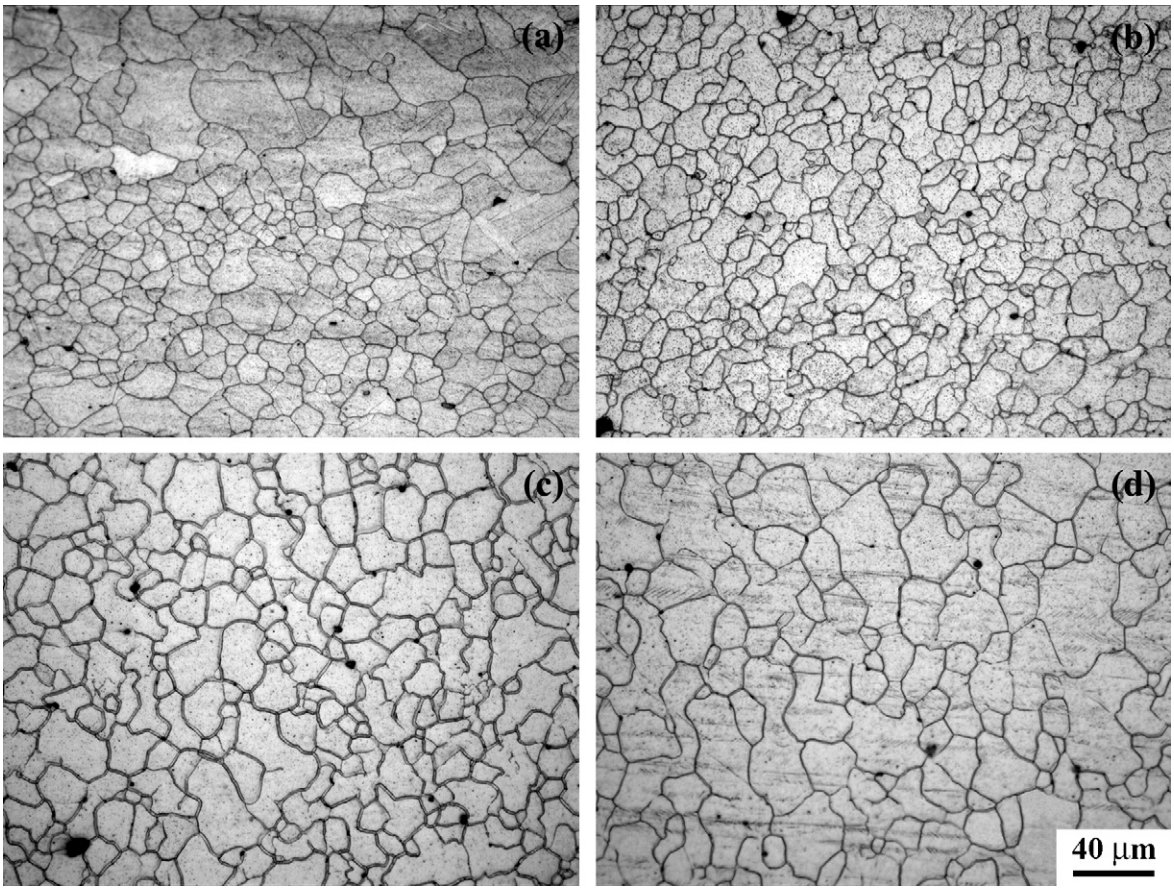

Fig. 3. Microstructure of FSW AZ31 joint: (a) base material, (b)–(d) sample 1–sample 3.

in the TMAZs differed slightly among the three samples, which was 13, 14 and 16 μm, respectively, for samples 1, 2, and 3 (Table 1). It seems that the grain size in the TMAZ was not much affected by the heat input of the shoulder. In this case, the grain size in the TMAZ was larger than that in the SZ for sample 1, whereas the TMAZ exhibited smaller grain size than the SZ for sample 3.

Fig. 5 shows the TEM images of the SZs of samples 1 and 3. It was revealed that there were dislocations within the recrystallized grains in the SZs and similar results were also observed in other studies [3,11]. Magnesium alloys are prone to undergo discontinuous DRX (DDRX) due to low stacking fault energy [18]. During DDRX, new grains nucleate at the subgrains, grain boundaries and dislocations. So the dislocation density would decrease. However, due to the continuous deformation during DDRX, some strain is retained in the new grains, making the dislocations accumulated in the recrystallized grains. Besides, Fig. 5 shows that samples 1 and 3 exhibited quite similar dislocation density in the SZs. It is believed that the deformation energy in the SZs during DRX is mainly related to the stirring of the threaded pin. The same pin size and weld parameter made the deformation energy similar for samples 1 and 3, producing similar dislocation density in the SZs.

3.2. Microtexture

The pole figures of the SZ and the BM are shown in Fig. 6. Similar to a previous report [14], the BM had a strong texture with the (0 0 0 2) plane perpendicular to the TD and ND. When the pin passed by, shear plastic flow made the material rotate around the pin column surface. The previous study [14] indicated that the (0 0 0 2) basal plane was distributed around the pin surface after FSW. The orientation of the basal plane (0 0 0 2) after FSW for different regions of the joints was reported by many studies [11,14,15]. They claimed that the basal plane (0 0 0 2) paralleled to the RD in the BM was switched to tilt to the TD in the transition zone and finally changed to parallel to the TD in the weld center. Similarly, in the present study, the texture in the SZ was significantly changed with the (0 0 0 2) plane having an inclination to the TD (Fig. 6). Besides, it is noted that samples 1, 2 and 3 exhibited similar texture orientation and intensity as shown in Fig. 6, indicating that the shoulder size change did not exert a significant effect on the texture in the SZs.

Fig. 7 shows the XRD results for the BM and the cross-section around the TMAZ in the FSW samples. The (0 0 0 2) peak in sample 1 was very strong, indicating that the (0 0 0 2) texture still existed. However, when the AZ31 plate was welded with a larger shoulder diameter of 24 mm (sample 3), the nearly random grain orientations were revealed since the three highest peaks had similar intensities. The present result is consistent with that obtained by Woo et al. [13]. It was reported that the shoulder size variation resulted in the change in the (0 0 0 2) texture distribution in the TMAZ of FSP AZ31 [13]. In a previous study of FSW AZ61 [15], the (0 0 0 2) basal plane around the TMAZ was found to have an inclination of ∼45° to the TD. As shown in the present study, sample 1 exhibited obvious texture in the TMAZ and could be more prone to slip with an orientation of ∼45° than sample 3 under the same condition.

3.3. Hardness profile

Fig. 8 shows the hardness profiles of samples 1, 2 and 3 along the mid-thickness of the plates. The hardness value of the BM fluctuated due to the inhomogeneous grain microstructure of the

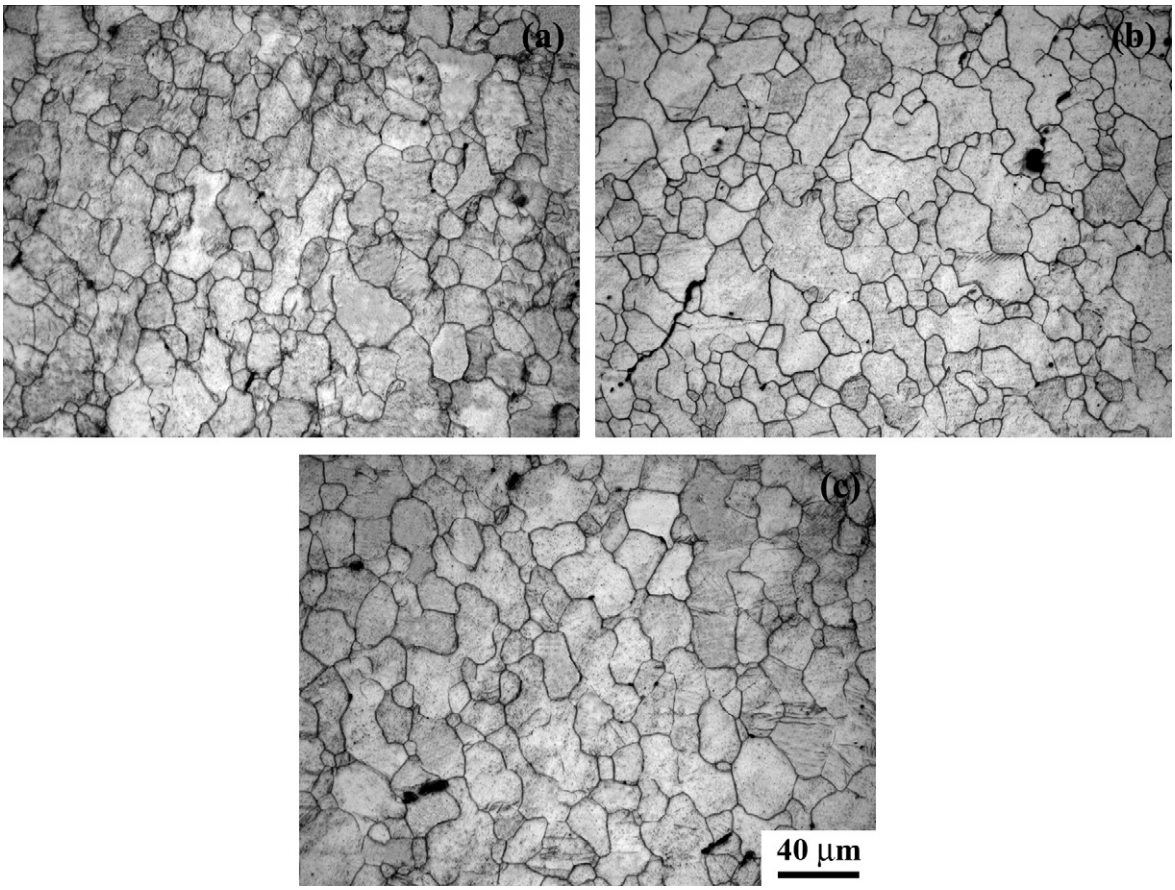

Fig. 4. Microstructure of FSW AZ31 joint in TMAZ of advanced side: (a)–(c) sample 1–sample 3.

as-rolled plate. The three FSW samples exhibited similar hardness profiles with the SZs having the hardness values of ~55 Hv, which was equivalent to the average hardness of the BM.

AZ31 alloy has few precipitation phases. Therefore, the hardness of the SZ is mainly governed by the gain size and dislocation density. However, in this study, the significant variation in the grain size did not exert a remarkable effect on the hardness profiles of the FSW joints. Similar results were also reported in recent studies [11,13]. The ratio of the grain sizes in the SZ and BM (d_{SZ}/d_{BM}) was 10 μm/21 μm and 19 μm/21 μm for samples 1 and 3 in this study, and was about 14 μm/25 μm and 17 μm/50 μm in Refs. [11,13], respectively. It is noted that the FSW AZ31 joints with this type of hardness profile had large grain size (>10 μm) in the SZ. In a previous study, Chang et al. [19] reported a Hall–Petch relationship between the hardness (H_V) and the grain size (d) for the SZ of friction stir processed (FSP) AZ31

$$H_V = 40 + 72\ d^{-1/2} \quad (1)$$

Similarly, Wang et al. [12] established a Hall–Petch relationship between the yield stress ($\sigma_{0.2}$) and the grain size for friction stir processed (FSP) AZ31

$$\sigma_{0.2} = 10 + 160\, d^{-1/2} \quad (2)$$

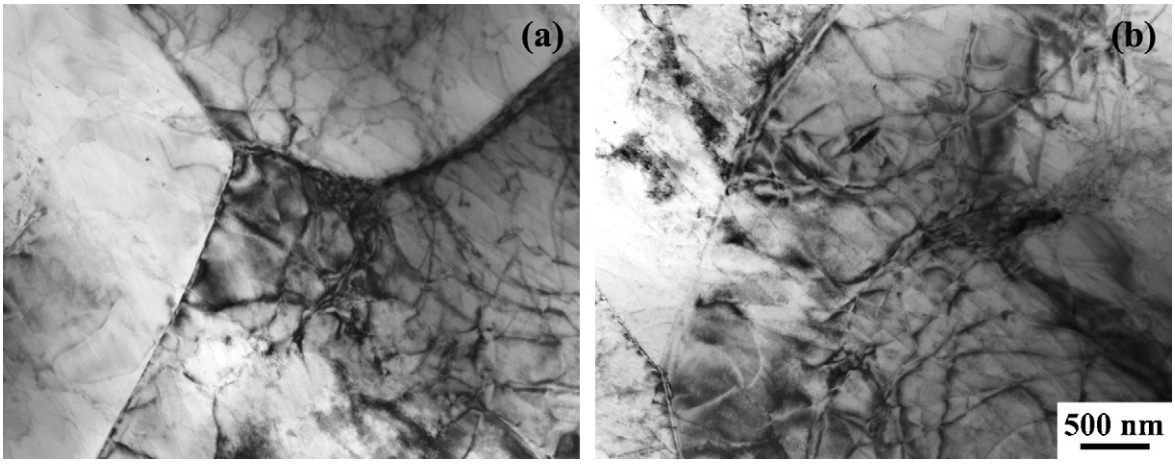

Fig. 5. TEM micrographs of stir zone: (a) sample 1 and (b) sample 3.

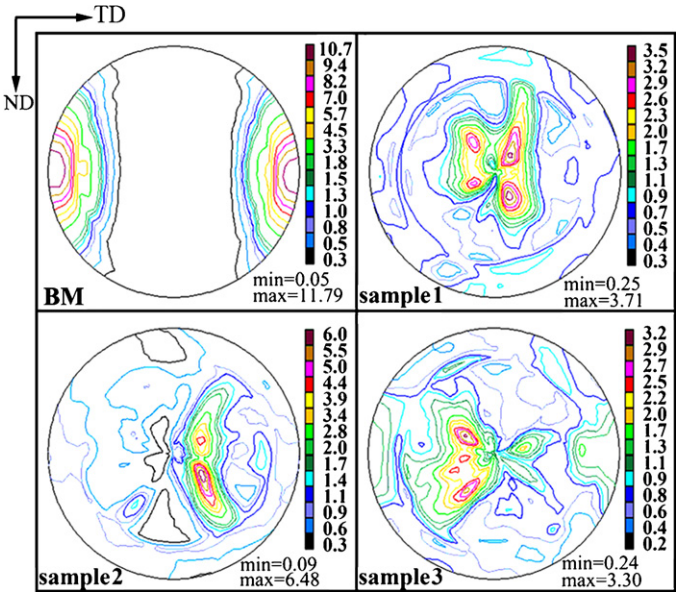

Fig. 6. XRD pole figures of base material and SZs on transverse plane of FSW AZ31 joints.

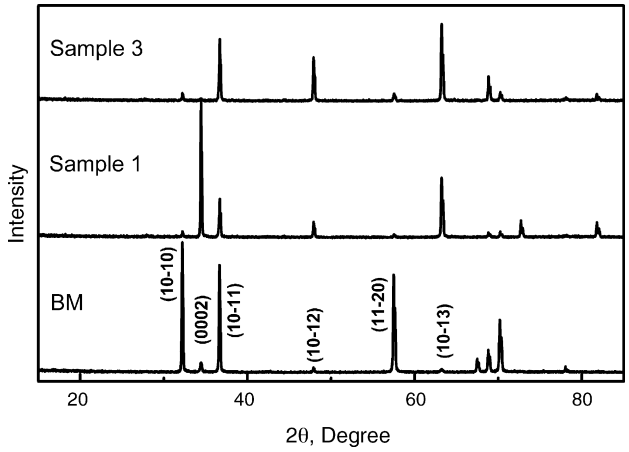

Fig. 7. XRD diffraction intensities of BM and TMAZs on transverse plane.

However, it should be pointed out that the grain size in the FSP AZ31 as reported by Chang et al. [19] and Wang et al. [12] was consistently smaller than ~8 μm. Furthermore, it was reported that when the grains in the SZ were refined to be smaller than 1 μm, the hardness increased rapidly [20]. These results indicated that the hardness values of the FSW AZ31 joints are insensitive to the grains size variation when the grain size is larger than 10 μm, whereas when the grain is further refined, for example, to below 8 μm, the hardness of the FSW AZ31 increases and follows the Hall–Petch relationship, as demonstrated by Chang et al. [19] and Wang et al. [12].

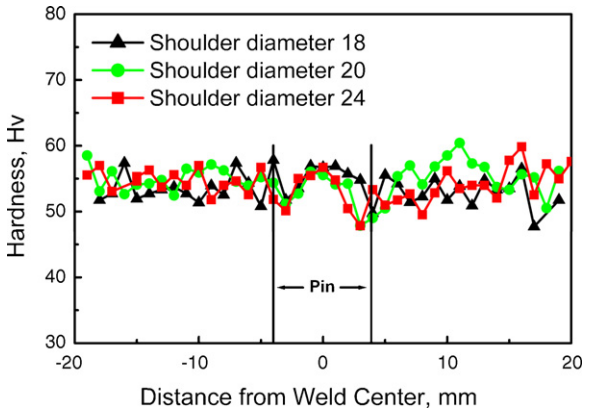

Fig. 8. Hardness profiles of FSW AZ31 joints along mid-thickness.

It is noted that with increasing the distance from the center of the SZs towards the TMAZs, the hardness decreased gradually, and the lowest hardness values were observed in the TMAZs at the advanced side for all FSW samples. As shown in Table 1, the grain size ratio in the TMAZ and SZ is 13 μm/10 μm, 14 μm/13 μm and 16 μm/19 μm, respectively. Clearly, the grains in the TMAZ were not always larger than those of the SZ for the three samples. Therefore, the lowest hardness in the TMAZ could not be explained by the variation in the grain size.

The hardness anisotropy has been found in many alloys [21]. Because the critical shear stress is different in different crystal planes and directions, the crystal orientation will exert an influence on the hardness values. During FSW, severe deformations occurred in the welded joint. As a result, a special orientation distribution was produced in the FSW magnesium alloy joints [15], i.e., the (0002) rotated around the stir pin, thereby producing the softest region around the TMAZ. So, the lowest hardness distribution observed in the TMAZ of the FSW AZ31 joints in the present study is associated with the crystal orientation.

In a previous study [11], the homogeneous hardness profile of the FSW AZ61 joint was attributed to the absence of significant differences in the dislocation density throughout the weld. The present TEM examinations indicated that the difference of dislocation density in the SZs between samples 1 and 3 was negligible, as shown in Fig. 5. This is consistent with the similar hardness values obtained in various SZs.

3.4. Tensile properties and fracture feature

The mechanical properties of the BM and FSW joints are shown in Table 2. Compared to those of the BM, both the strength and elongation of the FSW joints were significantly reduced. Similar results have been reported in the FSW AZ31 joints by other investigators [2–7]. It is noted that the joint efficiency tended to increase with increasing the shoulder size and the highest one of 86% was achieved in sample 3. This result is different from that observed in FSW aluminum alloys where smaller shoulder diameter produced better tensile properties in AA 6061 alloy [17]. Besides, the

Table 2
Tensile properties of mini specimens for stir zones and transverse specimens for FSW joints.

Sample no.	Mini specimen	Transverse tensile specimen				
	UTS, MPa	UTS, MPa	YS, MPa	El., %	Joint efficiency, %	Fracture location
1	253.2 ± 2.5	203.4 ± 1.1	104.4 ± 5.3	5.3 ± 0.1	81.5	TMAZ
2	–	207.2 ± 1.9	105.4 ± 1.3	5.9 ± 0.2	83.0	TMAZ
3	243.7 ± 4.3	215.6 ± 0.7	104.0 ± 1.1	10.7 ± 0.9	86.4	SZ
BM	258.2 ± 2.8	249.5 ± 0.8	153.0 ± 0.6	22.6 ± 0.4	–	–

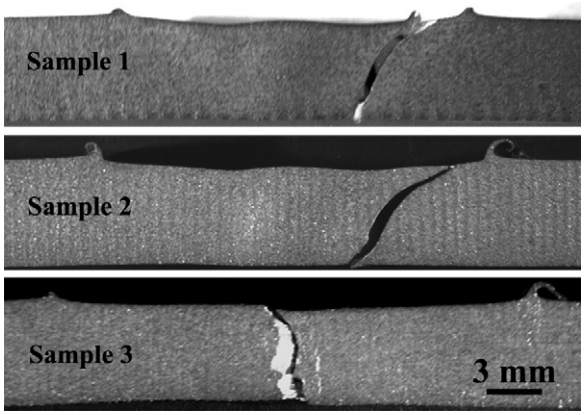

Fig. 9. Macroscopic images of failed friction stir welded AZ31 joints. (The advancing side of the weld is on the right.)

elongation of the FSW joints increased with increasing the shoulder diameter, especially an obviously enhanced elongation was obtained in sample 3. However, there was little variation in the yield strength of the joints with the variation in the shoulder diameters.

Fig. 9 shows the failed FSW joints. For samples 1 and 2, the fracture occurred in the TMAZs where obvious plastic deformation was detected, indicating lower strength in this region. This is in agreement with lower hardness in the TMAZs, as shown in Fig. 8. Furthermore, the sample thickness did not exhibit an obvious thinning, which is consistent with a lower elongation in two samples. However, increasing the shoulder diameter to 24 mm (sample 3) resulted in a shift of the fracture locations from the TMAZ to the SZ. This indicates that the weakest region of sample 3 was the SZ, rather than the TMAZs, which is contrary to lower hardness in the TMAZs of sample 3. This implies that the hardness is not the only factor to determine the strength of the magnesium alloys. Moreover, for sample 3, while the necking was not obvious at the fracture location, a noticeable thinning in the sample thickness in the SZ was observed, indicating large and homogeneous plastic deformation, which is consistent with a higher elongation of sample 3.

Mini tensile test indicated that the SZs of samples 1 and 3 exhibited a tensile strength of 253 and 244 MPa, respectively (Table 2). This variation trend is consistent with the variation in the grain size in the SZs (Table 1), but is contrary to that obtained by using large transverse tensile specimens. For sample 3, although the failure location shifted from the TMAZ with a grain size of 16 μm to the SZ with a grain size of 19 μm, the tensile strength increased compared to samples 1 and 2 with smaller grain sizes in the TMAZs (13–14 μm) and SZs (10–13 μm). Therefore, the improvement in the transverse tensile properties of the welds and the shift in the fracture location with increasing the shoulder diameter imply that the TMAZ in sample 3 was somewhat enhanced compared to that in samples 1 and 2, which could not be explained by the variation in the grain size in the TMAZs.

As a solid solution-strengthened alloy, the tensile properties of the FSW AZ31 joints are influenced by several factors, such as the grain size and dislocation density. In Fig. 5, the dislocation density in the SZ did not have noticeable differences between samples 1 and 3. Therefore, the difference in the tensile properties of the FSW samples could not be explained by the dislocation density. In some

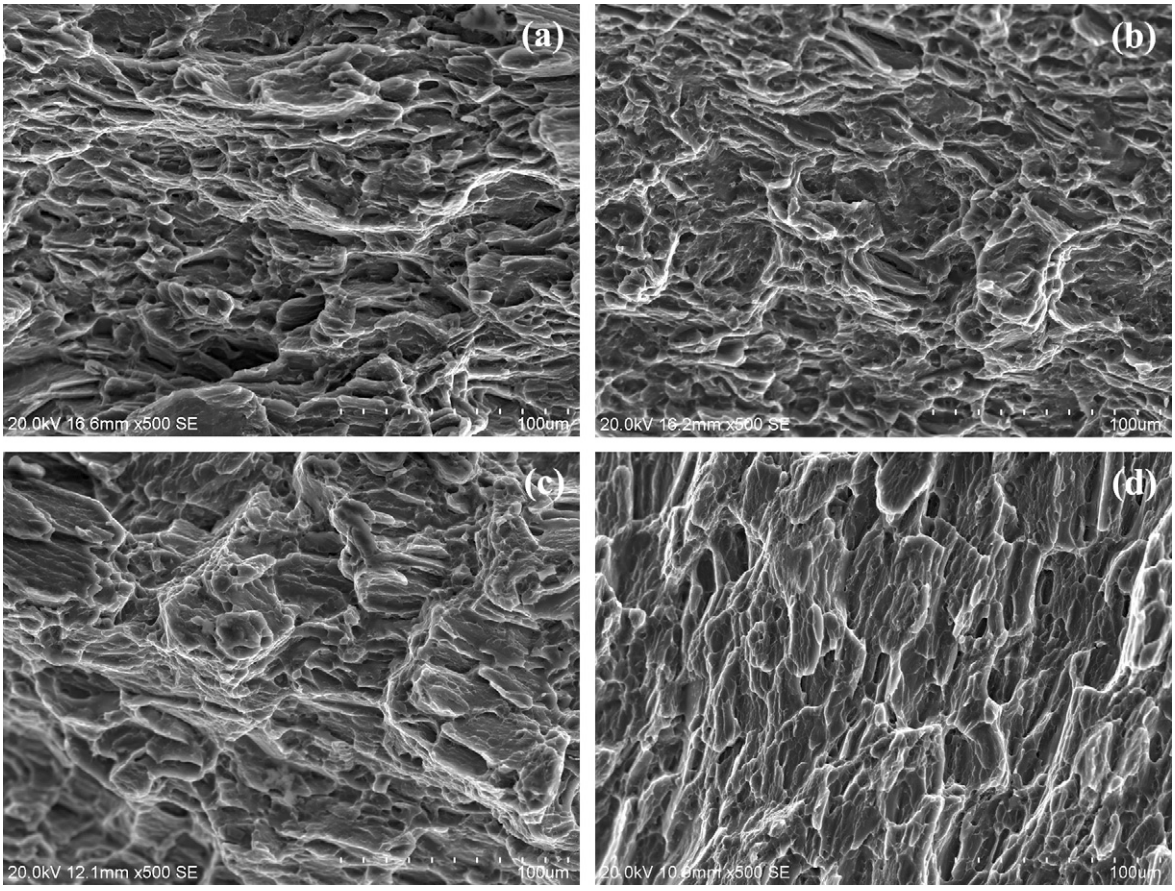

Fig. 10. SEM images showing facture surfaces: (a) BM, (b)–(d) sample 1–sample 3.

previous studies [4,5], the oxide layer in the boundary between the TMAZ and the SZ was considered as a reason for the failure of FSW AZ31 joints. However, in this study, no oxides were detected in the fracture surfaces of samples 1 and 2 that failed in the TMAZs. Tables 1 and 2 show that the UTS and the elongation of the FSW samples increased with increasing the grain size in the TMAZs and SZs, which resulted from the increase in the shoulder sizes. So in the present study, the texture patterns should be considered as a significant factor in controlling the tensile properties of the FSW joints.

As discussed above, the pole figures in the SZs were similar for these three FSW samples, indicating that the texture of the SZ was not a critical factor in influencing the strength of the welds. A previous study [15] found that the softest region was in the TMAZ for a FSW AZ61 joint. In the present study, a high intensity of (0 0 0 2) diffraction was found around the TMAZ for sample 1 and this made the material prone to slip along the (0 0 0 2) at low critical resolved shear stress. This is consistent with the obvious plastic deformation in the TMAZ of sample 1, as shown in Fig. 9. In this case, the strength of the TMAZ was lower than that of the SZ with the fracture occurring at the TMAZ for sample 1. By comparison, the TMAZ of sample 3 was enhanced due to nearly random texture in this region. In this case, the weak (0 0 0 2) diffraction intensity in the TMAZ made the strength of the TMAZ higher than that of the SZ, resulting in a shift in the fracture location from the TMAZ to the SZ. Because the SZ was obviously wider than the TMAZ, more homogeneous plastic deformation occurred in sample 3 than in sample 1, thereby producing larger elongation in sample 3.

The SEM micrographs of the fracture surfaces of the tensile specimens are shown in Fig. 10. The fracture surfaces consisted of tear ridges, dimples and cleavage facets for both the BM and the FSW samples, which show the quasi-cleavage crack feature, as reported in other magnesium alloys [22]. Besides, the tear ridges were elongated along a certain direction and the direction was different for the FSW samples and BM. It was found that the tear ridges of the BM was along the LD (Fig. 10a). However, some differences in the direction of the tear ridges were found when the heat input was increased. For the joints failed in the TMAZs, the tear ridges had little change (Fig. 10b and c), compared to the BM; whereas for sample 3 failed in the SZ, the direction of the tear ridges shifted to extend along the ND (Fig. 10d). Therefore, the change in the direction of the tear ridges would have some relations with the fracture locations.

Materials tend to crack along the crystal face with the weakest atomic binding forces in a quasi-cleavage crack, such as (0 0 0 2) basel plane of the magnesium alloys. As discussed above, the texture patterns are different in the TMAZ and SZ, this would make the tear ridge direction altered. For the rolled BM, the (0 0 0 2) plane along the LD and the direction of the tear ridges were along the same direction. For samples 1 and 2, the orientation of the (0 0 0 2) plane in the TMAZ just had a declination to the TD and did not have a large change compared to the SZ, and this orientation could make the tear ridges along the LD on the whole. However, for sample 3, the (0 0 0 2) plane was rotated around the pin in the SZ and it could make the tear ridges extend along the ND.

4. Conclusions

With increasing the shoulder diameter from 18 to 24 mm, the gains in the SZ increased remarkably, and the grains in the TMAZ exhibited a slight increase.

The three FSW samples exhibited similar hardness profiles along mid-thickness of the plates with the lowest hardness in the TMAZ on the advancing side.

The texture in the SZ was significantly changed with the (0 0 0 2) plane having an inclination to the TD, and the texture orientation and intensity was similar for the three FSW samples.

With a smaller shoulder 18 mm in diameter, the TMAZ exhibited a strong (0 0 0 2) texture, whereas with a larger shoulder 24 mm in diameter, nearly random grain orientation was observed in the TMAZ.

With increasing the shoulder diameter, the tensile strength of the joints tended to increase and the elongation was significantly improved, with the failure location of the joints shifting from the TMAZ to the SZ. Besides, the tear ridges in the fracture surface were changed from the TD to the ND. These are mainly attributed to the variation in the texture.

Acknowledgements

The authors gratefully acknowledge the support of (a) the National Outstanding Young Scientist Foundation of China under Grant no. 50525103 and (b) the Hundred Talents Program of Chinese Academy of Sciences.

References

[1] R.S. Mishra, Z.Y. Ma, Mater. Sci. Eng. R 50 (2005) 1–78.
[2] W.B. Lee, Y.M. Yeon, S.B. Jung, Mater. Sci. Technol. 19 (2003) 785–790.
[3] J.A. Esparza, W.C. Davis, E.A. Trillo, L.E. Murr, J. Mater. Sci. Lett. 21 (2002) 917–920.
[4] S. Lin, S. Kim, C.G. Lee, C.D. Yim, S.J. Kim, Metall. Mater. Trans. A 36A (2004) 1609–2005.
[5] N. Afrin, D.L. Chen, X. Cao, M. Jahazi, Mater. Sci. Eng. A 472 (2007) 179–186.
[6] L. Commin, M. Dumont, J.E. Masse, L. Barrallier, Acta Mater. 57 (2009) 326–334.
[7] M.A. Gharacheh, A.H. Kokabi, G.H. Daneshi, B. Shalchi Amirkhiz, R. Sarrafi, Int. J. Mach. Tool Manuf. 46 (2006) 1983–1987.
[8] G.M. Xie, Z.Y. Ma, L. Geng, R.S. Chen, Mater. Sci. Eng. A 471 (2007) 63–68.
[9] S. Mironov, Y. Motohashil, R. Kaibyshev, Mater. Trans. 48 (2007) 1387–1395.
[10] D.T. Zhang, M. Suzuki, K. Maruyama, Scr. Mater. 52 (2005) 899–903.
[11] S.H.C. Park, Y.S. Sato, H. Kokawa, Scr. Mater. 49 (2003) 161–166.
[12] Y.N. Wang, C.I. Chang, C.J. Lee, H.K. Lin, J.C. Huang, Scr. Mater. 55 (2006) 637–640.
[13] W. Woo, H. Choo, M.B. Prime, Z. Feng, B. Clausen, Acta Mater. 56 (2008) 1701–1711.
[14] W. Woo, H. Choo, D.W. Brown, P.K. Liaw, Z. Feng, Scr. Mater. 54 (2006) 1859–1864.
[15] S.H.C. Park, Y.S. Sato, H. Kokawa, Metall. Mater. Trans. A 34A (2003) 987–994.
[16] B.M. Darras, M.K. Khraisheh, F.K. Abu-Farha, M.A. Omar, J. Mater. Process. Technol. 191 (2007) 77–81.
[17] K. Elangovan, V. Balasubramanian, Mater. Des. 29 (2008) 362–373.
[18] F.J. Humphreys, M. Hatherly, Recrystallization and Related Annealing Phenomena, 1995, p. 371.
[19] C.I. Chang, C.J. Lee, J.C. Huang, Scr. Mater. 51 (2004) 509–514.
[20] C.I. Chang, X.H. Du, J.C. Huang, Scr. Mater. 57 (2007) 209–212.
[21] J.J. Vlassak, W.D. Nix, J. Mech. Phys. Solids 42 (1994) 1223–1245.
[22] Y. Yang, Y.B. Liu, Fatigue Fract. Eng. Mater. Struct. 30 (2007) 1149–1157.